Decentralized Safe Navigation for Multi-agent Systems via Risk-aware Weighted Buffered Voronoi Cells

Yiwei Lyu
Carnegie Mellon University
Pittsburgh, United States
yiweilyu@andrew.cmu.edu

John M. Dolan
Carnegie Mellon University
Pittsburgh, United States
jdolan@andrew.cmu.edu

Wenhao Luo
University of North Carolina at Charlotte
Charlotte, United States
wenhao.luo@uncc.edu

ABSTRACT

In this paper, we propose Risk-aware Weighted Buffered Voronoi tessellation, a variant of Generalized Voronoi tessellation, for decentralized multi-agent collision-free navigation. Inherited from the traditional Voronoi tessellation, a safety guarantee in terms of inter-robot collision avoidance is achieved by partitioning the joint state space of the multi-agent system into individual cells that constrain each individual agent's motion in a distributed manner. Different from many existing Voronoi tessellations-based collision avoidance approaches, our Risk-aware Weighted Buffered Voronoi Cell (Risk-aware WBVC) partition not only takes agent positional information into account, but also the motion information when determining the cell boundaries between pairwise robots. Our risk-aware WBVC relies on the novel use of Control Barrier Functions (CBF) as a measure of risk evaluation that captures to what extent the safety constraints are satisfied between pairwise robots. With that, the cell boundaries of risk-aware WBVC are determined by (1) the varying levels of relative efforts between pairwise agents to respond to potential collisions, and (2) the accumulated risk each agent experiences that is caused by the surrounding agents. This allows for an adaptive constrained space partition among robots that balances between individual's efforts in respecting the safety constraints and the overall threats due to other agents in the environment, e.g. an aggressive robot moving with higher speed requires a relatively larger space for responding to potential collisions, and a less-threatened robot may be expected to yield and make more room for those exposed to higher risk. Rigorous proofs of formal safety guarantees are provided and simulations are demonstrated on up to 16 robots to show the effectiveness of our method.

KEYWORDS

Safe Control; Multi-agent System; Collision Avoidance; Robotics

ACM Reference Format:
Yiwei Lyu, John M. Dolan, and Wenhao Luo. 2023. Decentralized Safe Navigation for Multi-agent Systems via Risk-aware Weighted Buffered Voronoi Cells. In *Proc. of the 22nd International Conference on Autonomous Agents and Multiagent Systems (AAMAS 2023), London, United Kingdom, May 29 – June 2, 2023*, IFAAMAS, 9 pages.

1 INTRODUCTION

Given their ability to accomplish large-scale tasks, multi-agent systems have been studied in a number of application domains, e.g. search and rescue [16], environmental sampling and exploration [10, 20], and precision agriculture [8]. To keep a multi-agent system safe, a collision-free configuration is required for every pairwise agent interaction in the system. In [3, 4] reciprocal velocity obstacles are used to control agents by assuming symmetric collision-avoidance reasoning of other agents. Safety barrier certificates have been explored to achieve collision-free motion by characterizing the joint admissible control space for the robot team [5, 22]. Methods in [6, 9] use Model Predictive Control-based methods for individual agent trajectory planning with receding horizons, treating all other agents as dynamic obstacles. However, these methods rely on an individual robot controller to constrain their own motion based on assumed behavior models of the surrounding robots and environments to achieve collision avoidance.

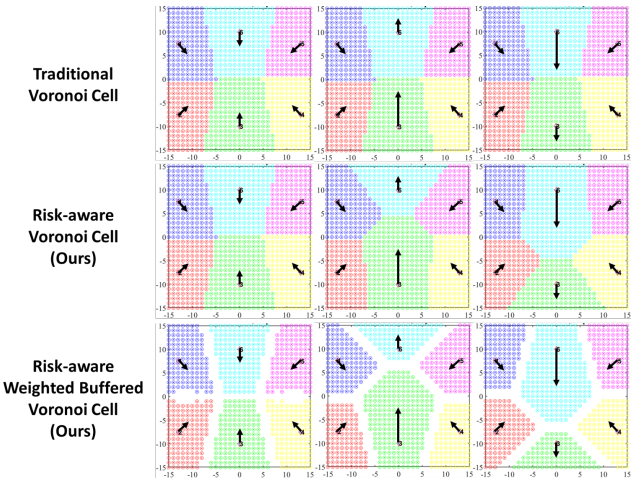

Figure 1: Our proposed Risk-aware Weighted Buffered Voronoi Cells v.s. traditional Voronoi Cells.

On the other hand, centralized control methods for multi-agent systems can be computationally expensive, and inter-agent communication may not be always available. Therefore, it is favorable to explore decentralized control approaches for multi-agent collision avoidance. Different approaches have been explored to translate centralized control into a decentralized setting, by splitting the constraints and separately solving individual optimization problems with split constraints, so that agents only need to make decisions based on local information, without the need to predict what others are going to do.

As a model-based approach, Control Barrier Functions (CBF) [1] is a powerful tool to ensure robot safety. It is widely applied as a

Proc. of the 22nd International Conference on Autonomous Agents and Multiagent Systems (AAMAS 2023), A. Ricci, W. Yeoh, N. Agmon, B. An (eds.), May 29 – June 2, 2023, London, United Kingdom.

constraint in optimization-based controllers to constrain the robot motion, so that as long as the robot is inside the defined safe set initially, then CBF can always ensure that the robot stays inside the safe set with formally provable guarantees [21, 22]. There have been some efforts in exploring decentralized CBF by splitting the joint admissible control space in different ways. [21] partitions the constraints based on agents' various actuation limits. [14, 19] demonstrate how to divide the constraints given the known information of agent social personalities, egoistic vs. altruistic.

Although decentralized CBF-based methods work well, they require all robots in the multi-agent system to use decentralized CBF-based controllers, and do not generalize well. To accommodate the possibility that agents may use different controllers, Voronoi Cell-based methods are more suitable. Voronoi Cells [25] have been extensively studied by partitioning the joint state space of the multi-agent system into individual cells, representing the admissible state space for each individual agent to avoid the collision. The space partition is conducted based on the spatial distance from a given point in the state space to each robot. However, we argue that agents with different motions should have different-sized cells. In this paper, we aim to build Risk-aware Weighted Buffered Voronoi Cells, in which risk refers to the likelihood of possible collision among agents. The intuition is that simply partitioning the state space based on the point-to-agent proximity, as existing Weighted Buffered Voronoi Cells do, cannot reflect the agent motion information well, which is quite crucial in collision avoidance. In other words, the risk of collision between any pairwise robots should not only depend on how close two agents are, but also on how fast they are moving towards each other. Therefore, our goal is to provide agents that pose higher risk to their neighboring agents with relatively larger cells to reflect the heterogeneity among agents, similar to the idea that a fully-loaded truck with higher speed needs a longer distance to stop.

To evaluate the risk from possible collision, we propose a Control Barrier Function (CBF)-inspired risk measurement that gives an agent situational awareness of the dynamic environment it is in from the CBF perspective. One advantage of our proposed CBF-inspired risk measurement is that the informativeness and expressiveness of CBF can be leveraged for risk evaluation, which characterizes pairwise agent safety based on various factors including agent positions, motion, and safety radius without requiring agents to actually carry the CBF-based controllers. Different from most existing works in which CBF is merely used as a binary verification of whether the system is still safe given the nominal control, in this work, our proposed CBF-inspired risk measurement characterizes to what extent the system is safe or unsafe, and then it is embedded into the Voronoi Cells partitioning to make the best use of the information CBF provides.

As a variant of traditional Voronoi Cells, Buffered Voronoi Cells have been introduced to account for agent safety radius or uncertainty [19, 23, 25, 26] and are widely applied in multi-agent collision avoidance. In Weighted Buffered Voronoi Cells (WBVC), the boundaries of the adjacent cells are biased in a certain way so that the space between two agents is not divided equally. Since our focus is to construct the Weighted Buffered Voronoi Cells in a risk-aware manner, different from other works that only concern safety between pairwise robots, we argue that in order to better characterize an agent's collision risk, only considering the effect of its neighboring agents is not enough. We also need to consider the neighbors of the neighbors. An example is, for an agent at the center of a crowd being surrounded and another agent at the edge of the crowd, although the pairwise safety requirements are both satisfied, the agent surrounded by the crowd faces higher risk. Therefore, another advantage of our CBF-inspired risk measurement is that it can take the aggregated risk into consideration, so that the cell boundaries are biased towards agents with less relative aggregated risk, leaving them a more constrained state space to proceed with extra caution, with the awareness regarding the existence of its riskier neighbor.

Our **main contributions** are: **1)** We present a CBF-inspired risk measurement to quantify the cumulative risk the agents face in a crowded dynamic environment, especially for multi-agent interaction scenarios; **2)** We propose Risk-aware Weighted Buffered Voronoi Cells (Risk-aware WBVC), which partitions the joint state space of the robot teams and biases the cell boundaries based on CBF-inspired risk measurement, making it generally applicable and extremely suitable for multi-agent decentralized collision avoidance maneuvers; **3)** We provide rigorous proofs on the formal safety guarantee our Risk-aware Weighted Buffered Voronoi tessellation brings, and validate the proposed method in multi-agent collision avoidance scenarios with up to 16 robots.

2 PRELIMINARIES

2.1 Background of Control Barrier Function

Control Barrier Functions (CBF) [1] are used to define an admissible control space for the safety assurance of dynamical systems. One of its important properties is its forward-invariance guarantee of a desired safety set. Consider a nonlinear system in control affine form: $\dot{x} = f(x) + g(x)u$, where $x \in \mathcal{X} \subset \mathbb{R}^n$ and $u \in \mathcal{U} \subset \mathbb{R}^m$ are the system state and control input with f and g assumed to be locally Lipschitz continuous. A desired safety set $\mathcal{H}$ can be denoted by a safety function $h(x)$: $\mathcal{H} = \{x \in \mathbb{R}^n : h(x) \geq 0\}$. Thus the control barrier function for the system to remain in the safety set can be defined as follows [1]:

Definition 2.1. (Control Barrier Function) Given the aforementioned dynamical system and the set $\mathcal{H}$ with a continuously differentiable function $h : \mathbb{R}^n \to \mathbb{R}$, then h is a control barrier function (CBF) if there exists a class $\mathcal{K}$ function for all $x \in \mathcal{X}$ such that

$$\sup_{u \in \mathcal{U}} \{\dot{h}(x, u)\} \geq -\kappa\big(h(x)\big) \tag{1}$$

We selected the same class $\mathcal{K}$ function $\kappa(h(x)) = \gamma h(x)$ as in [7, 12, 24], where $\gamma \in \mathbb{R}^{\geq 0}$ is a CBF design parameter controlling system behaviors near the boundary of $h(x) = 0$. Hence, the admissible control space in (1) can be redefined as $\mathcal{B}(x) = \{u \in \mathcal{U} : \dot{h}(x, u) + \gamma h(x) \geq 0\}$. It is proved in [1] that any controller $u \in \mathcal{B}(x)$ will render the safe state set $\mathcal{H}$ forward-invariant, i.e., if the system starts inside the set $\mathcal{H}$ with $x(t = 0) \in \mathcal{H}$, then it implies $x(t) \in \mathcal{H}$ for all $t > 0$ under controller $u \in \mathcal{B}(x)$.

2.2 Weighted Buffered Voronoi Cell

[*Summarized from* [19]] Consider a bounded, convex environment $Q \subset \mathbb{R}^n$, with individual points $q \in Q$. Within the environment,

there are N agents, with the positions of each agent denoted $p_i \in Q$ for $i = \{1, ..., N\}$. Each agent is assumed to have integrator dynamics,

$$\dot{p_i} = u_i \tag{2}$$

where u_i is the nominal control input for agent i.

The standard Voronoi Partition is defined as:

$$V_i = \{q \in Q | \|q - p_i\|^2 \leq \|q - p_j\|^2, \forall j \neq i, \quad i, j \leq N\} \tag{3}$$

where V_i denotes the cell of each agent i. Boundaries between cells are determined based on the Euclidean distance between q and the agents. Therefore, the boundary perpendicularly and equally divides the space between the neighboring agents, leaving them the same distances to the shared boundary.

The Weighted Voronoi Partition is defined as:

$$V_i = \{q \in Q | \|q - p_i\|^2 - \omega_i \leq \|q - p_j\|^2 - \omega_j\} \tag{4}$$

where ω_i and ω_j are the weights of each agent, and the Voronoi boundary is moved towards the agent with the larger weight.

The Buffered Voronoi Partition is defined as:

$$V_i = \{q \in Q | \|q - p_i\|^2 \leq \|q - p_j\|^2 - \omega_{ij}\} \tag{5}$$

where ω_{ij} defines the cell weightings between agent i and neighbors $j \in \mathcal{N}_i$, creating gaps between agent boundaries as a safety radius buffer. Buffered Voronoi Cells are usually used to guarantee agents will not collide when situated on their boundaries [2, 25].

3 METHOD

3.1 Control Barrier Function (CBF)-inspired Risk Measurement

Since we are interested in pairwise agent safety, we define the pairwise safety function $h_{ij}(p)$ and safety set $\mathcal{H}$ as:

$$\mathcal{H}(p) = \{p \in \mathcal{P} : \ h_{ij}(p) = ||p_i - p_j||^2 - r_{safe}^2 \geq 0, \forall i \neq j\} \tag{6}$$

$p_i, p_j \in \mathbb{R}^2$ for $i, j = \{1, ..., N\}$ are the positions of any pairwise agents i and j, and $r_{safe} = r_i + r_j$ is the required minimum pairwise safety distance considering both agents' safety radius. The admissible control space for each set of pairwise agents is: $\mathcal{B}_{ij}(p) = \{u \in \mathcal{U} : \dot{h}_{ij}(p, u) \geq -\gamma(h_{ij}(p))\}$. Inspired by CBF, we define our pairwise safety loss function $L_{ij}(p, u) \in \mathbb{R}$ as follows:

$$L_{ij}(p, u) = -\dot{h}_{ij}(p, u) - \gamma h_{ij}(p) - c \tag{7}$$

where c as a constant offset is a very large positive value to ensure $L_{ij}(p, u)$ is always negative to prevent unintended cancel-out when being accumulated later. $u_i, u_j \in \mathbb{R}^2$ are the agents' velocities. The safety loss function $L_{ij}(p, u)$ represents how close the system is to the boundary of the safe set, or how easily a safety violation could occur, under the assumption that both agents move with piecewise-constant velocity [13].

$L_{ij}(p, u)$ describes the risk agent i faces as the potential safety loss when interacting with agent j. For a multi-agent system, the aggregated risk agent i faces posed by surrounding agents $R_i \in \mathbb{R}$ is therefore defined as:

$$R_i = \phi(\sum_{j=1}^{N} L_{ij}(p, u)), \quad \forall j \neq i \tag{8}$$

where $\phi(\cdot) \in \mathbb{R} \mapsto \mathbb{R}$ is a mapping function that maps the value of R_i to the range $[0, 1]$. The larger R_i is, the more likely a safety violation is to occur. The proposed risk measurement is simple yet effective: 1) R_i grows with the increased number of agents in the system, as the environment becomes more complex and challenging; 2) R_i varies depending on the changes of states, including positions and motion of other agents as we expected, as it is important to tell how much risk agent i is exposed to even when a collision has not happened yet.

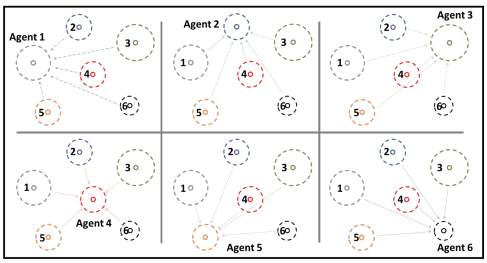

Figure 2: Propagated risk evaluation for individuals in a multi-agent system. Each arrow represents the risk posed by the pairwise relative movement of the evaluated agent and its neighboring agent.

Fig. 2 provides an illustrative example of how risk is calculated for individual agents in a multi-agent interaction scenario. For all six robots, the risk each individual agent faces consists of the pairwise risk generated by the surrounding five agents.

Note that the proposed CBF-inspired risk measurement does not necessarily require the agents to use CBF-based controllers. We understand that in the real world, agents may use different kinds of controllers, yet it does not prevent them from understanding the risk generated from multi-agent interaction from the CBF perspective, with the mild but reasonable assumption that information about agent states and safety margins are known or observable.

3.2 Risk-aware Weighted Buffered Voronoi Cells (Risk-aware WBVC)

To incorporate the risk measurement information in the Voronoi Cells partition, we extend the Control Barrier Function-inspired risk measurement to any individual point q in the state space being evaluated, by assuming that it is occupied by a static agent with zero velocity. In this way, Eq. 7 and 8 can be generalized from the original agent-to-agent risk measurement to agent-to-point risk measurement.

Definition 3.1. In a bounded, convex environment $Q \in \mathbb{R}^n$, for any individual point $q \in Q$ and each agent i with $p_i \in Q$ for $i = \{1, ..., N\}$, the cell V_i of agent i is a **Risk-aware Voronoi Cell**, if

$$V_i = \{q \in Q | \|L_{qi}\| \leq \|L_{qj}\|, \forall j \neq i, \quad i, j \leq N\} \tag{9}$$

where $L_{(\cdot)}$ is the pairwise safety loss function calculated in Eq.7.

Different from traditional Voronoi Cells, we use agent-to-point safety loss function $L_{(\cdot)}$ instead of point-to-point Euclidean Distance, to partition the state space based on the amount of risk

agents i and j generate on the individual point q. Therefore, the agent which brings the surrounding environment higher risk has a larger cell.

Definition 3.2. In a bounded, convex environment $Q \in \mathbb{R}^n$, for any individual point q with $p_q \in Q$ and each agent i with $p_i \in Q$ for $i = \{1, ..., N\}$, the cell W_i of agent i is a **Risk-aware Weighted Voronoi Cell**, if

$$\begin{aligned} W_i &= \{q \in Q | \|L_{qi}\| - \omega_i \leq \|L_{qj}\| - \omega_j, \quad \forall j \neq i, \quad i, j \leq N\} \\ \omega_i &= \frac{1}{2}(p_i - p_j)^T(u_i + u_j) + \frac{1}{4}(R_i - R_j) \cdot \|(p_i - p_j)^T(u_i - u_j)\| \\ \omega_j &= -\omega_i \end{aligned} \tag{10}$$

where $L_{(\cdot)}$ is the pairwise safety loss function calculated in Eq.7 and $R_{(\cdot)}$ is the accumulated risk over the individual agents calculated in Eq.8. $p_{(\cdot)}$ and $u_{(\cdot)}$ are agent position and velocity. $\gamma \in \mathbb{R}$ is the CBF design parameter.

By embedding CBF-inspired accumulated risk measurement into the weight design, the direction of the weight bias is decided based on the relative accumulated risk agent i and j received. Compared to agent j, the larger the relative accumulated risk agent i receives from the rest of the group, the larger weight ω_i it has, and the further the boundary between agent i and j is pushed towards j. To take agent safety radius into account, a buffer is added to the cell boundaries to ensure safety while agents are situated on the boundaries:

Definition 3.3. In a bounded, convex environment $Q \in \mathbb{R}^n$, for any individual point q with $p_q \in Q$ and each agent i with $p_i \in Q$ for $i = \{1, ..., N\}$, the cell W_i of agent i is a **Risk-aware Weighted Buffered Voronoi Cell**, if

$$\begin{aligned} W_i &= \{q \in Q | \|L_{qi}\| \leq \|L_{qj}\| - \omega_{ij}, \quad \forall j \neq i, \quad i, j \leq N\} \\ \omega_{ij} &= \|r_i + r_j\| \cdot \|\gamma(p_i - p_j) + (u_i - u_j)\| - (p_i - p_j)^T(u_i + u_j) \\ &+ [1 - \frac{1}{2}(R_i - R_j)] \cdot \|(p_i - p_j)^T(u_i - u_j)\| \end{aligned} \tag{11}$$

where $L_{(\cdot)}$ is the pairwise safety loss function calculated in Eq.7 and $R_{(\cdot)}$ is the accumulated risk over the individual agents calculated in Eq.8. $r_{(\cdot)}$ is agent safety radius, $p_{(\cdot)}$ and $u_{(\cdot)}$ are agent position and velocity. γ is the CBF design parameter.

With the weight design ω_{ij} shown in Eq. 11, a gap between cells with a minimum distance of $(r_i + r_j)$ is added between adjacent cells. Note that when CBF parameter $\gamma = 1$ and $u_i = u_j = 0$, the Risk-aware Weighted Buffered Voronoi Cell and weighting degrade to the traditional Voronoi Cell and Voronoi weighting [2, 25], which considers positional information only.

3.3 Safety Guarantee of Risk-aware WBVC

We propose that a multi-agent system can achieve formally provable safety guarantees in collision avoidance by utilizing the proposed Risk-aware WBVC. In this section, we prove that with Risk-aware Weighted Buffered Voronoi Cells, agents are guaranteed not to collide.

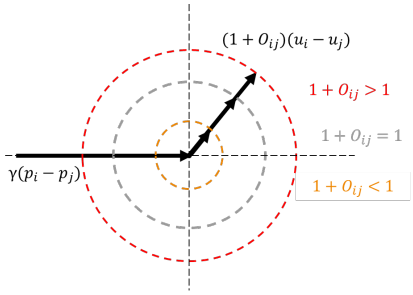

Figure 3: A geometric illustration of the inequality in Eq. 12.

Definition 3.4. In a multi-agent system of N agents, the configuration of agents is collision-free if the distances $\|p_i - p_j\|$ of all pairwise agents i and j satisfy

$$\|p_i - p_j\| \geq (r_i + r_j), \quad \forall i, j \in \{1, ..., N\}, i \neq j \tag{12}$$

where p_i, p_j are agent positions and r_i, r_j are agent safety radii.

Now we prove that for any agents in Risk-aware Weighted Buffered Voronoi Cells in collision-free configurations, 1) the cell of each agent is guaranteed to be non-empty; 2) the minimum distance between any two cells is guaranteed to satisfy the collision-free configuration requirement; and 3) the cells of Risk-aware WBVC are non-overlapping.

Lemma 3.5. *(Non-empty Cells). For each agent i with position p_i and cell W_i, $W_i \neq \emptyset$ when the agents are in a collision-free configuration.*

Proof. To prove the property of cell non-emptiness, we aim to prove that for any agent i, its position p_i always belongs to W_i. By Def. 3.3, substitute $q = p_i$ and we have:

$$\begin{aligned} &-\gamma(r_i + r_j)^2 \leq 2(p_j - p_i)^T u_j + \gamma[(p_j - p_i)^2 - (r_i + r_j)^2] - \omega_{ij} \\ &\Rightarrow (p_i - p_j)^T[\gamma(p_i - p_j) - 2u_j] - \omega_{ij} \geq 0 \\ &\Rightarrow (p_i - p_j)^T[\gamma(p_i - p_j) + (u_i - u_j) - (u_i + u_j)] - \omega_{ij} \geq 0 \end{aligned} \tag{13}$$

Substituting ω_{ij} defined in Def. 3.3 into the equation above, we have

$$\begin{aligned} &(p_i - p_j)^T[\gamma(p_i - p_j) + (1 + O_{ij})(u_i - u_j)] \\ &\geq (r_i + r_j)\|\gamma(p_i - p_j) + (u_i - u_j)\| \end{aligned} \tag{14}$$

where $O_{ij} = [1 - \frac{1}{2}(R_i - R_j)] \cdot \text{sign}[(p_i - p_j)^T(u_i - u_j)] \in \mathbb{R}$. It is straightforward that Eq. 14 always holds true. A geometric illustration is demonstrated in Fig. 3 for easier understanding. The black arrow on the left denotes the vector $\gamma(p_i - p_j)$, and the black arrows on the right denote the vector $(1 + O_{ij})(u_i - u_j)$ with possibly different values of $(1 + O_{ij})$. The dashed circles represent the regions vector $(1 + O_{ij})(u_i - u_j)$ is in corresponding to different values of $(1 + O_{ij})$. Since $\|p_i - p_j\| \geq (r_i + r_j)$ always stays true with the collision-free configuration, it is illustrative that, if we can prove that the projection magnitude of vector $(\gamma(p_i - p_j) + (1 + O_{ij})(u_i - u_j))$ along the direction of vector $(p_i - p_j)$ is always greater than or equal to that of vector $(\gamma(p_i - p_j) + (u_i - u_j))$ along the direction of vector $(p_i - p_j)$, then the inequality always stays

true. Note that the two vectors $(\gamma(p_i - p_j) + (1 + O_{ij})(u_i - u_j))$ and $(\gamma(p_i - p_j) + (u_i - u_j))$ share the same starting point. The ending point of $(\gamma(p_i - p_j) + (u_i - u_j))$ lies on the grey dashed circle, and the ending point of $(\gamma(p_i - p_j) + (1 + O_{ij})(u_i - u_j))$ lies on the red, grey or yellow dashed circle, depending on the value of $(1 + O_{ij})$. Now this problem boils down to the comparison of two projections. As shown in Fig. 3, when the vector $(u_i - u_j)$ is in the half-plane on the right (when $(p_i - p_j)^T(u_i - u_j) > 0$), $O_{ij} = [1 - \frac{1}{2}(R_i - R_j)] \cdot \text{sign}[(p_i - p_j)^T(u_i - u_j)] > 1$, the ending point of $(\gamma(p_i - p_j) + (1 + O_{ij})(u_i - u_j))$ lies in the right half-plane of the red dashed circle, and the projection magnitude of $(\gamma(p_i - p_j) + (1 + O_{ij})(u_i - u_j))$ is greater than that of $(\gamma(p_i - p_j) + (u_i - u_j))$. This statement also holds true when the vector $(u_i - u_j)$ is in the half-plane on the left (when $(p_i - p_j)^T(u_i - u_j) < 0$), $O_{ij} = [1 - \frac{1}{2}(R_i - R_j)] \cdot \text{sign}[(p_i - p_j)^T(u_i - u_j)] < 0$, meaning the ending point of $(\gamma(p_i - p_j) + (1 + O_{ij})(u_i - u_j))$ lies in the left half-plane of the yellow dashed circle. If the vector $(u_i - u_j)$ sits on the vertical half-planes' boundary, the two projections' magnitude is the same. Thus, it is proved that no matter where the vector $(u_i - u_j)$ lies, it is always guaranteed that Eq. 14 stays true. Therefore, the cells in Risk-aware WBVC $W_i \neq \emptyset$.

□

Lemma 3.6. *(Minimum Distance between Cells). For agent i and j with Cells W_i and W_j, any two random points $\bar{p}_i \in W_i$ and $\bar{p}_j \in W_j$, $\|\bar{p}_i - \bar{p}_j\| \geq (r_i + r_j)$.*

Proof. Given Def. 3.3, considering $q = \bar{p}_i$ and $\bar{p}_j$ respectively, we have

$$\begin{aligned}
&\|-2(p_i - \bar{p}_i)^T(u_i - \bar{u}_i) - \gamma((p_i - \bar{p}_i)^2 - (r_i + r_j)^2) - c\| \leq \\
&\|-2(p_j - \bar{p}_i)^T(u_j - \bar{u}_i) - \gamma((p_j - \bar{p}_i)^2 - (r_i + r_j)^2) - c\| - \omega_{ij} \\
&\|-2(p_j - \bar{p}_j)^T(u_j - \bar{u}_j) - \gamma((p_j - \bar{p}_j)^2 - (r_i + r_j)^2) - c\| \leq \\
&\|-2(p_i - \bar{p}_j)^T(u_i - \bar{u}_j) - \gamma((p_i - \bar{p}_j)^2 - (r_i + r_j)^2) - c\| - \omega_{ji}
\end{aligned} \tag{15}$$

By adding the two equations together, we have

$$-2(\bar{p}_i - \bar{p}_j)^T[\gamma(p_i - p_j) + (u_i - u_j)] \leq -(\omega_{ij} + \omega_{ji}) \tag{16}$$

The sum of the two weightings is

$$\omega_{ij} + \omega_{ji} = 2\|r_i + r_j\| \cdot \|\gamma(p_i - p_j) + (u_i - u_j)\| + 2\|(p_i - p_j)^T(u_i - u_j)\| \tag{17}$$

Substituting this expression into Eq. 16, this reduces to

$$\begin{aligned}
&(\bar{p}_i - \bar{p}_j)^T[\gamma(p_i - p_j) + (u_i - u_j)] \\
&\geq \|r_i + r_j\| \cdot \|\gamma(p_i - p_j) + (u_i - u_j)\| + \|(p_i - p_j)^T(u_i - u_j)\|
\end{aligned} \tag{18}$$

For two vectors a and b, it is known that $\|a\|\|b\| > \|a^T b\|$. Let $a = (\bar{p}_i - \bar{p}_j)$ and $b = [\gamma(p_i - p_j) + (u_i + u_j)]$; we can then state

$$\begin{aligned}
\|\bar{p}_i - \bar{p}_j\| &\geq \frac{(\bar{p}_i - \bar{p}_j)^T[\gamma(p_i - p_j) + (u_i - u_j)]}{\|\gamma(p_i - p_j) + (u_i - u_j)\|} \\
&\geq \frac{\|r_i + r_j\| \cdot \|\gamma(p_i - p_j) + (u_i - u_j)\| + \|(p_i - p_j)^T(u_i - u_j)\|}{\|\gamma(p_i - p_j) + (u_i - u_j)\|} \\
&= (r_i + r_j)(1 + \frac{\|(p_i - p_j)^T(u_i - u_j)\|}{\|\gamma(p_i - p_j) + (u_i - u_j)\|}) \\
&\geq \|r_i + r_j\|
\end{aligned} \tag{19}$$

thus proving that $\|\bar{p}_i - \bar{p}_j\| \geq (r_i + r_j)$ for any two points $\bar{p}_i \in V_i$ and $\bar{p}_j \in V_j$, for all $i \neq j$.

□

Lemma 3.7. *(Non-overlapping Cells). For a point $\bar{p}_i$ belonging to W_i, then $\bar{p}_i \notin W_j$ for all $j \neq i$, and $W_i \cap W_j = \emptyset$.*

Proof. For a point $q \in W_i$, it must satisfy the cell definition in Def. 3.3:

$$\|L_{qi}\| \leq \|L_{qj}\| - \omega_{ij} \tag{20}$$

Assuming $q \in W_j$ is true at the same time, by definition we have

$$\begin{aligned}
\|L_{qj}\| &\leq \|L_{qi}\| - \omega_{ji} \\
&\leq \|L_{qj}\| - \omega_{ij} - \omega_{ji} \\
0 &\leq -2\|r_i + r_j\| \cdot \|\gamma(p_i - p_j) + (u_i - u_j)\| - 2\|(p_i - p_j)^T(u_i - u_j)\|
\end{aligned} \tag{21}$$

From this contradiction, it is proved that $q \notin W_j$. Since any point within a cell cannot belong to any other cell at the same time, we conclude that $W_i \cap W_j = \emptyset, \forall i \neq j$. □

3.4 Collision-free Navigation with Risk-aware WBVC

We have proved in the previous section that, with our proposed Risk-aware WBVC, being collision-free is ensured when agents are within their own cells. With our three proven Risk-aware WBVC properties, it is straightforward and has been proved in [19] (Theorem 1) that, for agents navigating towards target positions which are located outside the cells, projecting the goal positions inside the cells can always guarantee collision-free navigation performance.

Now we present our algorithm for multi-agent safe navigation utilizing the proposed Risk-aware Weighted Buffered Voronoi Cells in Algorithm 1.

where $\bar{g}_i$ is the desired goal position of agent i, and $\hat{g}_i$ is the projected goal position if the goal is outside the cell W_i. g_i^* is the goal position fed into a move-to-goal controller or any other kind of controller that drives the robot to move towards the goal. With our proposed algorithm, while the goal has not been reached, the agent will first calculate L_{ij} and R_i with our CBF-inspired risk measurement. By updating the Risk-aware Weighted Buffered Voronoi Cells, the heterogeneity among agents in terms of different levels of risk exposure and risk generation ability is reflected in different sizes and shapes of the cells.

Algorithm 1 Safe Navigation in Risk-aware WBVC

Require: Collision-free $p(t_0), u(t_0), \bar{g}, \quad \forall i \in \{1, ..., N\}$
  while $\|\bar{g}_i - p_i\| > 0, \quad \forall i \in \{1, ..., N\}$ **do**
    Calculate pairwise safety loss function L_{ij} (Eq. 7)
    Calculate the accumulated risk R_i (Eq. 8)
    Update weights ω_{ij} (Def. 3.3)
    Update Voronoi Cell Tessellation W_i (Def. 3.3)
    if $\bar{g}_i \in W_i$ **then**
      Set $g_i^* = \bar{g}_i$
    else
      Find intersection $\hat{g}_i$ of the cell boundary and the connecting line between p_i and $\bar{g}_i$
      Set $g_i^* = \hat{g}_i$
    end if
    Update control policy $\dot{p}_i = -k(g_i^* - p_i)$
  end while

4 SIMULATION & DISCUSSION

In this section, we demonstrate the validity and effectiveness of the proposed method in multi-agent swapping games. The goal is for pairwise agents to switch positions with each other without any collision. We set the agent safety radius as $0.2m$ and the right-hand heuristic is applied for deadlock resolution [15, 18]. We demonstrate our method in two scenarios of 6 and 16 agents respectively. The agents have unicycle dynamics, and we employ a nonlinear inversion method [17] to map the desired velocity to the unicycle dynamics of mobile robots without compromising the safety guarantee [11].

4.1 Comparison with Traditional Voronoi Cells

In the first example, we consider a multi-agent system with six robots. To demonstrate the effectiveness of Risk-aware WBVC, the difference between our proposed tessellation and the traditional Voronoi tessellation is compared on a static configuration. The comparison is shown in Fig. 1. The three rows correspond to traditional Voronoi Cells, Risk-aware Voronoi Cells and Risk-aware Weighted Buffered Voronoi Cells. The cells of the six agents are marked in different colors and the black arrows indicate the velocity of the agents with different magnitudes and directions. The agents in all plots share the same positions, but with different velocity settings corresponding to the three columns.

In the first row, we can see that since the tessellation is conducted solely based on positional information and does not take agent motion into account, no matter where the agents are heading and how fast they are moving, the cells are equally partitioned. In the second row, we use the proposed CBF-inspired risk measurement to take not only agent position but also motion into account for tessellation, without any weight or buffer. We can see that the sizes and shapes of the cells change when the agent takes different actions. Since we are not partitioning the space based on the point-to-agent euclidean distance, the shared cell boundaries are no longer perpendicular to the line between neighboring agents. This makes sense, since if we take agent motion into consideration, the generated risk is higher in the direction it moves than in the opposite direction, and it is therefore unnecessary to leave the same large cell space behind the agent. Our proposed Risk-aware WBVC is presented in the third row, and we observe that the lower the risk the agent poses to its surrounding environment compared to its neighboring agents, the smaller its cell is, warning it of the presence of its dangerous neighbor. The higher the risk the agent is exposed to, the larger cell it is given to grant it additional space for safe maneuvers. We further demonstrate the effectiveness of our Risk-aware WBVC in Fig. 7, in which the positions of all agents are fixed and the agent velocities are randomized. From the 10 randomized trials, it is shown that our proposed Risk-aware WBVC can better reflect the risk quantified via the CBF-based risk measurement, compared to the traditional Weighted Buffered Voronoi Cells that will have the same and equal cells.

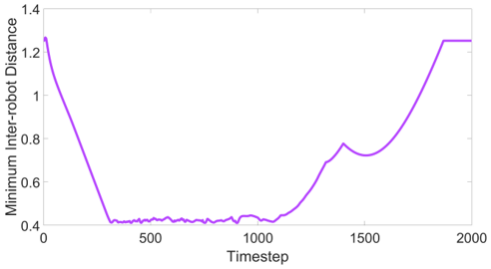

Figure 4: The minimum inter-robot distance among 6 robots.

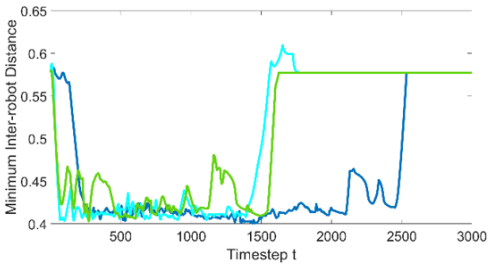

Figure 5: The minimum inter-robot distance among 16 robots.

4.2 Safety Performance in Collision Avoidance

Next, we demonstrate the safety performance of our proposed Risk-aware WBVC. We first show the six-agent position swapping game in Fig. 8. The numbers in black are agent indices and the numbers in red are target position indices, indicating to which agent they belong. We observe that the agents are able to dynamically compute and update their Voronoi Cells in a risk-aware manner. The inter-robot distance over time is recorded in Fig. 4. The y-axis represents the minimum inter-agent distance. Since we set the safety radius of individual agents to be $0.2m$, the minimum inter-agent distance should be larger than or equal to $0.4m$. The plot shows that the safety requirement is satisfied in the six-agent position-swapping game.

In the second example, we consider a more complicated and challenging environment with 16 robots in total. We ran 3 trials with randomly assigned pairwise counterparts for agents to swap positions. Due to the space limit, we only demonstrate the swapping process of one trial in Fig. 9. For better visualization, we separately show agent trajectories in Fig. 6. The minimum inter-robot distance over time of the 3 trials is shown in Fig. 5, with the green line

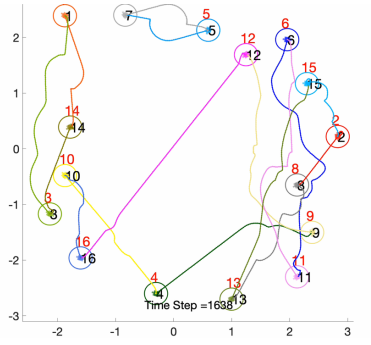

Figure 6: Trajectories of sixteen robots.

corresponding to the demo case in Fig. 9. It is observed that no safety violation happens during the whole process and the agents are able to safely navigate to their target positions. The risk evaluation is conducted and the risk measurement is leveraged to update the Weighted Buffered Voronoi Cells in a risk-aware manner.

4.3 Tunable Overall Risk Sensitivity

Compared to traditional Voronoi Cells that only compute cells based on positional information, by quantifying risk from a CBF perspective, our proposed Risk-aware WBVC also characterizes various levels of the overall risk sensitivity of the multi-agent system.

It is demonstrated in Fig. 10 that for a given set of agent positions and velocities, by tuning the CBF design parameter γ, the Risk-aware WBVC is computed with different levels of risk tolerance. The smaller γ is, the more conservative the multi-agent system behaves, and the larger γ is, the more aggressive the overall system is. For higher overall risk sensitivity, extra cautions are taken by the multi-agent system by adaptively enlarging gaps in between the cells for enhanced safety performance.

Note that different levels of system aggressiveness or conservativeness in our Risk-aware WBVC are not equivalent to simply using larger or smaller buffers in traditional Weighted Buffered Voronoi Cells (WBVC). In our Risk-aware WBVC, the cells' shapes and sizes are also different, characterizing the possible heterogeneity of the overall risk sensitivity. Mathematically γ serves as a balancing parameter between the influence of the positional information and the motion information in cell partitioning, and the larger γ is, the closer Risk-aware WBVC is to traditional WBVC. As mentioned previously, our Risk-aware WBVC is a generalized version of traditional WBVC, and it degrades to traditional WBVC when $\gamma = 1$ and the agent motion information is set to zero when computing cells, which is also verified in the proof of Lemma 2 that our Risk-aware WBVC provides a tight lower bound on the minimum distance between cells compared to that of traditional WBVC.

5 CONCLUSION

In this paper, we propose the Risk-aware Weighted Buffered Voronoi Cells (Risk-aware WBVC), which utilizes novel Control Barrier Function-inspired risk measurement to evaluate the risk each individual agent faces and the accumulated risk from inter-agent interaction. Rigorous proofs are provided for formally provable guarantees for multi-agent collision-free navigation with our Risk-aware WBVC. The effectiveness and safety performance of the proposed approach is demonstrated in multi-agent position-swapping games with up to sixteen robots. For future work, we aim to extend Risk-aware WBVC for safe navigation under uncertainty.

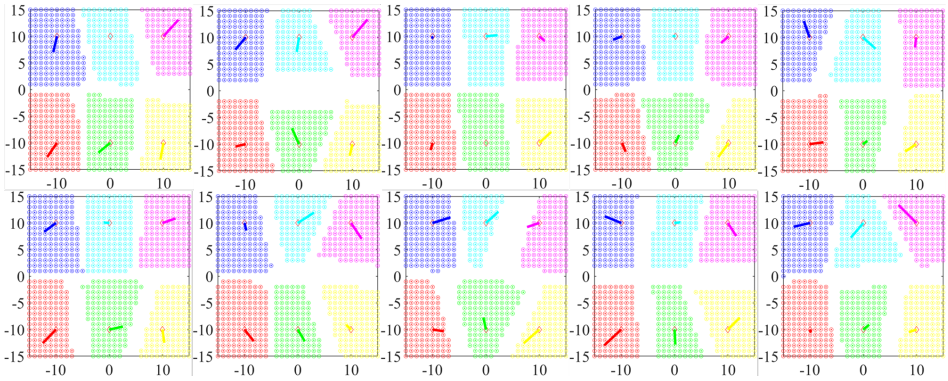

Figure 7: Risk-aware WBVC with randomized agent velocities at the same positions. The colorful lines represent the randomized agent velocities with different magnitudes and directions.

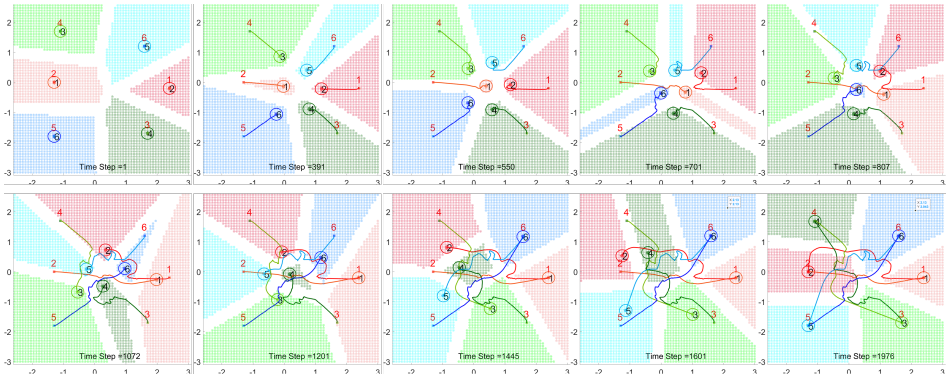

Figure 8: Our proposed Risk-aware Weighted Buffered Voronoi Cell in a 6-robot position swapping game.

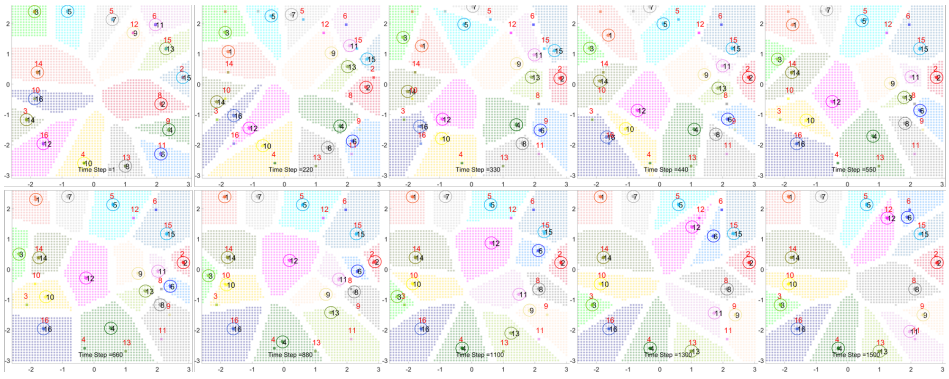

Figure 9: Our proposed Risk-aware Weighted Buffered Voronoi Cell in a 16-robot position swapping game.

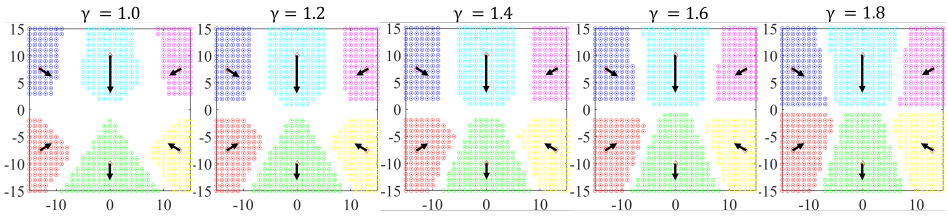

Figure 10: Different levels of multi-agent system's sensitivity to risk. The smaller γ is, the more sensitive the multi-agent system is to risk and therefore extra cautions are taken when computing Risk-aware WBVC.

REFERENCES

[1] Aaron D Ames, Samuel Coogan, Magnus Egerstedt, Gennaro Notomista, Koushil Sreenath, and Paulo Tabuada. 2019. Control barrier functions: Theory and applications. In *2019 18th European control conference (ECC)*. IEEE, 3420–3431.

[2] Saptarshi Bandyopadhyay, Soon-Jo Chung, and Fred Y Hadaegh. 2014. Probabilistic swarm guidance using optimal transport. In *2014 IEEE Conference on Control Applications (CCA)*. IEEE, 498–505.

[3] Daman Bareiss and Jur Van Den Berg. 2015. Generalized reciprocal collision avoidance. *The International Journal of Robotics Research* 34, 12 (2015), 1501–1514.

[4] Andrew Best, Sahil Narang, and Dinesh Manocha. 2016. Real-time reciprocal collision avoidance with elliptical agents. In *IEEE International Conference on Robotics and Automation (ICRA)*. 298–305.

[5] Urs Borrmann, Li Wang, Aaron D Ames, and Magnus Egerstedt. 2015. Control barrier certificates for safe swarm behavior. *IFAC-PapersOnLine* 48, 27 (2015), 68–73.

[6] Noel E Du Toit and Joel W Burdick. 2011. Robot motion planning in dynamic, uncertain environments. *IEEE Transactions on Robotics* 28, 1 (2011), 101–115.

[7] Suiyi He, Jun Zeng, Bike Zhang, and Koushil Sreenath. 2021. Rule-Based Safety-Critical Control Design using Control Barrier Functions with Application to Autonomous Lane Change. arXiv:2103.12382 [eess.SY]

[8] Wajahat Kazmi, Morten Bisgaard, Francisco Garcia-Ruiz, Karl Damkjær Hansen, and Anders la Cour-Harbo. 2011. Adaptive surveying and early treatment of crops with a team of autonomous vehicles. In *Proceedings of the 5th European Conference on Mobile Robots ECMR 2011*. 253–258.

[9] Björn Lindqvist, Sina Sharif Mansouri, Ali-akbar Agha-mohammadi, and George Nikolakopoulos. 2020. Nonlinear MPC for collision avoidance and control of UAVs with dynamic obstacles. *IEEE robotics and automation letters* 5, 4 (2020), 6001–6008.

[10] Wenhao Luo, Shehzaman S Khatib, Sasanka Nagavalli, Nilanjan Chakraborty, and Katia Sycara. 2016. Distributed knowledge leader selection for multi-robot environmental sampling under bandwidth constraints. In *IEEE/RSJ International Conference on Intelligent Robots and Systems (IROS)*. IEEE, 5751–5757.

[11] Wenhao Luo, Wen Sun, and Ashish Kapoor. 2020. Multi-robot collision avoidance under uncertainty with probabilistic safety barrier certificates. *Advances in Neural Information Processing Systems* 33 (2020), 372–383.

[12] Yiwei Lyu, Wenhao Luo, and John M Dolan. 2021. Probabilistic safety-assured adaptive merging control for autonomous vehicles. In *IEEE International Conference on Robotics and Automation (ICRA)*. 10764–10770.

[13] Yiwei Lyu, Wenhao Luo, and John M Dolan. 2022. Adaptive safe merging control for heterogeneous autonomous vehicles using parametric control barrier functions. In *2022 IEEE Intelligent Vehicles Symposium (IV)*. IEEE, 542–547.

[14] Yiwei Lyu, Wenhao Luo, and John M Dolan. 2022. Responsibility-associated Multi-agent Collision Avoidance with Social Preferences. In *2022 IEEE 25th International Conference on Intelligent Transportation Systems (ITSC)*. IEEE, 3645–3651.

[15] Ahmed Nazeem, Spyros Reveliotis, Yin Wang, and Stéphane Lafortune. 2011. Designing Compact and Maximally Permissive Deadlock Avoidance Policies for Complex Resource Allocation Systems Through Classification Theory: The Linear Case. *IEEE Trans. Automat. Control* 56, 8 (2011), 1818–1833. https://doi.org/10.1109/TAC.2010.2095612

[16] James Parker, Ernesto Nunes, Julio Godoy, and Maria Gini. 2016. Exploiting spatial locality and heterogeneity of agents for search and rescue teamwork. *Journal of Field Robotics* 33, 7 (2016), 877–900.

[17] Daniel Pickem, Paul Glotfelter, Li Wang, Mark Mote, Aaron Ames, Eric Feron, and Magnus Egerstedt. 2017. The robotarium: A remotely accessible swarm robotics research testbed. In *2017 IEEE International Conference on Robotics and Automation (ICRA)*. IEEE, 1699–1706.

[18] Alyssa Pierson and Daniela Rus. 2017. Distributed target tracking in cluttered environments with guaranteed collision avoidance. In *2017 International Symposium on Multi-Robot and Multi-Agent Systems (MRS)*. IEEE, 83–89.

[19] Alyssa Pierson, Wilko Schwarting, Sertac Karaman, and Daniela Rus. 2020. Weighted buffered voronoi cells for distributed semi-cooperative behavior. In *IEEE international conference on robotics and automation (ICRA)*. 5611–5617.

[20] Tomáš Rouček, Martin Pecka, Petr Čížek, Tomáš Petříček, Jan Bayer, Vojtěch Šalanskỳ, Daniel Heřt, Matěj Petrlík, Tomáš Báča, Vojěch Spurnỳ, et al. 2019. Darpa subterranean challenge: Multi-robotic exploration of underground environments. In *International Conference on Modelling and Simulation for Autonomous Systems*. Springer, 274–290.

[21] Li Wang, Aaron Ames, and Magnus Egerstedt. 2016. Safety barrier certificates for heterogeneous multi-robot systems. In *American Control Conference (ACC)*. 5213–5218.

[22] L. Wang, A. D. Ames, and M. Egerstedt. 2017. Safety Barrier Certificates for Collisions-Free Multirobot Systems. *IEEE Transactions on Robotics* 33, 3 (2017), 661–674.

[23] Mingyu Wang and Mac Schwager. 2019. Distributed collision avoidance of multiple robots with probabilistic buffered voronoi cells. In *2019 international symposium on multi-robot and multi-agent systems (MRS)*. IEEE, 169–175.

[24] Jun Zeng, Bike Zhang, and Koushil Sreenath. 2021. Safety-critical model predictive control with discrete-time control barrier function. In *2021 American Control Conference (ACC)*. IEEE, 3882–3889.

[25] Dingjiang Zhou, Zijian Wang, Saptarshi Bandyopadhyay, and Mac Schwager. 2017. Fast, on-line collision avoidance for dynamic vehicles using buffered voronoi cells. *IEEE Robotics and Automation Letters* 2, 2 (2017).

[26] Hai Zhu, Bruno Brito, and Javier Alonso-Mora. 2022. Decentralized probabilistic multi-robot collision avoidance using buffered uncertainty-aware Voronoi cells. *Autonomous Robots* 46, 2 (2022), 401–420.